2021年11月11日(木)

A会場

インターナショナル sess.

[1A09-10] インターナショナル sess.(1)

座長:村山 徹(東京都立大学)
13:00 ～ 14:00 A会場 (函館アリーナ 会議室A)

[1A09] 【招待】脱水素的な分子転換プロセスの開発 –アルコール電解からメタン多量化まで–

○荻原 仁志[1] （1. 埼玉大学）

13:00 ～ 13:30

[1A10] [Invited] Precise synthesis, characterization, and reactivity of multi-functional catalysts

○Ro Insoo[1] （1. Seoul National University of Science and Technology）

13:30 ～ 14:00

インターナショナル sess.

[1A11-13] インターナショナル sess.(2)

座長:比護 拓馬(早稲田大学)
14:15 ～ 15:00 A会場 (函館アリーナ 会議室A)

[1A11] ゼオライト内インジウムヒドリド種の局所構造とエタン脱水素化能

○安村 駿作[1]、鳥屋尾 隆[1,2]、前野 禅[1]、清水 研一[1,2] （1. 北海道大学触媒科学研究所、2. 京都大学触媒電池）

14:15 ～ 14:30

[1A12] Au-Pt/ゼオライトを用いた0℃における高効率エチレン除去

○Lin Mingyue[1]、Wang Haifeng[1]、宍戸 哲也[1]、三浦 大樹[1]、春田 正毅[1]、村山 徹[1,2] （1. 東京都立大学、2. 煙台大学）

14:30 ～ 14:45

[1A13] Catalytic reduction of NO to ammonia by CO-H_2O over metal oxide supported catalysts

○Chaudhari Chaudhari Chandan[1], Keisuke Kobayashi[1], Yuichi Manaka[1,2], Tetsuya Nanba[1] （1. Fukushima Renewable Energy Inst., AIST , 2. Tokyo Inst. Tech. ）

14:45 ～ 15:00

インターナショナル sess.

[1A14-16] インターナショナル sess.(3)

座長:桑原 泰隆(大阪大学)
15:15 ～ 16:00 A会場 (函館アリーナ 会議室A)

[1A14] Low-temperature conversion of methane to methanol using carbon nanotubes supported catalyst

○Yingluo He[1], Guohui Yang[1], Noritatsu Tsubaki[1] （1. University of Toyama）

15:15 ～ 15:30

[1A15] CO_2吸着用 HKUST-1モノリスのワンポット合成

○酒井 求[1]、堀 隼太[2]、伊藤 綾香[3]、松本 隆也[4]、朝野 剛[4]、松方 正彦[1,2,3,5] （1. 早稲田大学ナノ・ライフ創新研究機構、2. 早稲田大学大学院先進理工学研究科応用化学専攻、3. 早稲田大学先進理工学部応用化学科、4. ENEOS株式会社、5. 早稲田大学理工学術院総合研究所）

15:30 ～ 15:45

[1A16] 火炎噴霧熱分解法により調製した Zr添加 Ni/CeO_2のCO_2メタン化反応活性

○藤原 翔[1]、樋野 宗悟[1]、吉岡 大[2] （1. 山形大学大学院　理工学研究科、2. 山形大学　工学部）

15:45 ～ 16:00

インターナショナル sess.

[1A09-10] インターナショナル sess.(1)

座長:村山 徹(東京都立大学)

2021年11月11日(木) 13:00 〜 14:00 A会場 (函館アリーナ 会議室A)

[1A09] 【招待】脱水素的な分子転換プロセスの開発　–アルコール電解からメタン多量化まで–

○荻原 仁志[1]（1. 埼玉大学）

13:00 〜 13:30

[1A10] [Invited] Precise synthesis, characterization, and reactivity of multi-functional catalysts

○Ro Insoo[1]（1. Seoul National University of Science and Technology）

13:30 〜 14:00

Dehydrogenative conversion of small molecules – from alcohol electrolysis to methane polymerization

(Saitama Univ.) ○ Hitoshi Ogihara

1. Introduction

The conversions of small molecules to value-added chemicals are important processes in the chemical industry. This presentation will show several dehydrogenative conversions processes. One is the electrolysis of lower alcohols. We have developed electrolysis systems for the conversion of lower alcohols into esters, aldehydes, and acetals.[1,2] The feature of the system is to use membrane electrode assembly (MEA) as an electrolysis unit. As shown in Fig. 1, alcohols converted into esters, aldehydes, and acetals on the anode. Then, proton and electron transfer through a proton-exchange membrane (PEM) and an external circuit, respectively. Finally, the proton and electron are recombined on the cathode to generate hydrogen. The electrolysis using MEA can be a sustainable process for upgrading alcohols to chemicals because it can use renewable electricity and does not require chemical reagents (e. g., oxidants and electrolytes).

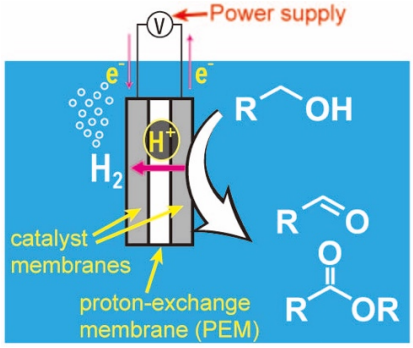

Fig. 1 Schematic diagram of electrolysis of alcohols using an MEA unit

Furthermore, we also studied the direct conversion of methane (CH_4) to C2 hydrocarbons and aromatics. CH_4 is expected to be used to produce essential chemicals, and recent developments in shale gas extraction technology are also supporting the use of natural gas in the chemical industry. However, CH_4, which is the main component of natural gas, is highly stable due to its strong C–H bond and symmetric molecular structure, making it difficult to convert it into useful chemicals. In this presentation, some approaches to activate CH_4 molecules are reported.

2. Results and Discussion

2.1 Electrolysis of alcohols using an MEA unit

We have proposed processes to convert alcohols into chemicals via the dehydrogenative electrolysis using an MEA device. One example is the electrolysis of methanol (CH_3OH). We found that the electrolysis of pure CH_3OH using the MEA device selectively produced methyl formate,[1] which is an important intermediate in the production of essential chemicals. The methyl formate and hydrogen are directly formed from CH_3OH according to Eqs 1 and 2. The average formation rate of methyl formate was 930 mmol h^{-1} g_{cat}^{-1} and a turnover frequency was 468 h^{-1}. The productivity of methyl formate via pure CH_3OH electrolysis was comparable to previously reported systems such as heterogeneous catalysts and photocatalysts.

$$\text{Anode:}\quad 2CH_3OH \rightarrow HCOOCH_3 + 4H^+ + 4e^- \qquad (1)$$
$$\text{Cathode:}\quad 2H^+ + 2e^- \rightarrow H_2 \qquad (2)$$

Next, we focused on ethanol (C_2H_5OH). The electrolysis of ethanol showed different behavior from CH_3OH electrolysis. In the electrolysis of pure C_2H_5OH, the main product was 1,1-diethoxyethane (DEE).[2] The formation scheme is shown in Fig. 2. Unlike CH_3OH, the electrochemical reaction of C_2H_5OH is mainly produced acetaldehyde as follows:

$$C_2H_5OH \rightarrow CH_3CHO + 2H^+ + 2e^- \qquad (3)$$

where a Pt/C acted as an electrocatalyst, then, acetaldehyde is converted into DEE with the aid of PEM (Nafion, in this study). Nafion is known as a strong acid catalyst so that the Nafion promotes the following acetalization reaction.

$$CH_3CHO + 2C_2H_5OH \rightarrow CH_3CH(OC_2H_5)_2 + H_2O \qquad (4)$$

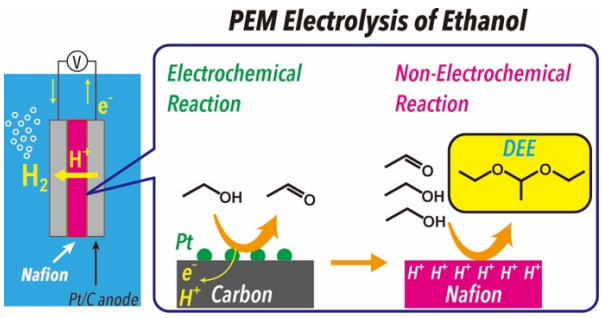

Fig. 2 Electrolysis of ethanol to form DEE.

DEE was produced at high faradaic efficiency (78 %) via the sequential electrochemical and nonelectrochemical reactions. The DEE formation rate was higher than that of previous reported systems.

So far, MEA has been widely used in the field of fuel cells and water electrolysis. Our work proposed that the MEA can be used as the electrolysis unit for upgrading alcohols into value-added chemicals (e.g., esters, aldehydes, and acetals).

2.2 Dehydrogenative polymerization of CH_4

Catalytic decomposition of CH_4 is a reaction that produces COx-free hydrogen.

$$CH_4 \rightarrow 2H_2 + C \quad (5)$$

We investigated the catalytic activity Pd-M alloy on the decomposition of CH_4 and found that Pd-Au and Pd-Si alloys promoted not only the decomposition of CH_4 but also coupling of CH_4 to produce C2 hydrocarbons.[3,4)]

$$2CH_4 \rightarrow C_2H_6 + H_2 \quad (6)$$

$$2CH_4 \rightarrow C_2H_4 + 2H_2 \quad (7)$$

Although the selectivity for C2 hydrocarbons was not so high (~2%), this is the first report that valuable C2 hydrocarbons can be co-produced during the decomposition of CH_4 to produce COx-free hydrogen.

In addition to the catalytic process, we proposed a new radical route to activate CH_4.[5)] CH_4 is so stable molecule that it cannot be activated without catalysts even at high temperatures. As shown in Table 1, CH_4 was not converted at 800 °C in the absence of catalysts. In contrast, ethane (C_2H_6) is more reactive than CH_4; therefore, C_2H_6 was dehydrogenated into C_2H_4 and C_6H_6 etc. In such a case, CH_4 is expected to be an inert gas; however, mixtures of CH_4/C_2H_6 and of Ar/C_2H_6 showed different pyrolysis behaviors; the addition of CH_4 increased the formation of propylene, propane and toluene. To reveal the activation process of CH_4, we used ^{13}C-labeled CH_4. Mass spectrometry analysis showed that carbon contained in CH_4 was incorporated into the pyrolysis products. We assumed that CH_4 was attacked by radical species generated from pyrolysis of C_2H_6 and was converted into methyl radicals (Fig. 3). The CH_4-derived methyl radicals were incorporated into pyrolysis products via radical reactions.

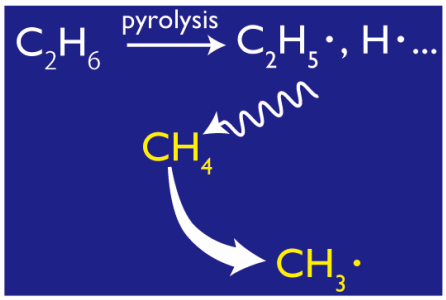

Fig. 3 Schematic diagram of CH_4 activation by radicals generated from the pyrolysis of C_2H_6.

3. Acknowledgement

This work was supported by JSPS KAKENHI (Grant Number 16K18287, 18K04832, and 21H01710), JST CREST (Grant Number JPMJCR15P4), the technology development project carried out in Japan Petroleum Energy Center (JPEC) under the commission of the Ministry of Economy, Trade and Industry (METI), and Tonen General Sekiyu Research/Development Encouragement & Scholarship Foundation.

References:

1) R. Kishi, H. Ogihara, M. Yoshida-Hirahara, K. Shibanuma, I. Yamanaka, H. Kurokawa, *ACS Sustain. Chem. Eng.*, **2020,** 8, 11532–11540.

2) D. Kawaguchi, H. Ogihara, H. Kurokawa, *ChenSusChem*, in press.

3) H. Ogihara, N. Imai, M. Yoshida-Hirahara, H. Kurokawa, *Chem. Lett.*, **2020**, 49, 236-239.

4) H. Ogihara, N. Imai, H. Kurokawa, *Int. J. Hydrog. Energy*, **2020**, 45, 33612-33622.

5) H. Ogihara, H. Tajima, H. Kurokawa, *React. Chem. Eng.*, **2020** ,48, 1145-1147.

Table 1 dehydrogenative conversion of CH_4, C_2H_6, and CH_4/C_2H_6. T = 1073 K, catalyst mass = 0 g.

reactant gas	yield / μmol h^{-1}								conv. / %	
	C_2H_4	C_2H_2	C_3H_8	C_3H_6	C_6H_6	C_7H_8	C_8H_8	$C_{10}H_8$	CH_4	C_2H_6
CH_4	1	n.d.	n.d.	n.d.	n.d.	n.d.	n.d.	n.d.	0.002	n/a
Ar/C_2H_6	13027	303	2	113	192	0.9	2	10	n/a	90.6
CH_4/C_2H_6	13611	266	24	595	125	3	2	4	-0.7	85.0

Precise Synthesis, Characterization, and Reactivity of Multi-functional Catalysts

Seoul National University of Science and Technology
Insoo Ro *

1. Introduction

Beyond the maximized atomic efficiencies and cost savings, atomically dispersed catalysts have attracted great attention in recent years due to the uniformity in active sites and careful regulation over local environments of active sites. Thus, it is interesting to investigate how the dispersed active site-support environment can be precisely engineered to control catalytic reactivity. In this work, we demonstrate control over the local coordination environment of atomically dispersed Rh on Al_2O_3 through a systematic tuning of interactions between Rh and ReO_x or WO_x species. Through this precise engineering of the local environment of atomically dispersed Rh species on an oxide support, it is shown that the local environment of the active site are significantly influenced, which in turn control ethylene hydroformylation reactivity. Whereas ReO_x were atomically dispersed on Al_2O_3 regardless of Re loading, the structure of WO_x on Al_2O_3 varied (atomically dispersed WO_x, polystungstate monolayer, to monoclinic WO_3 crystallites) by changing W loading, which influences the intrinsic reaction kinetics.

2. Experimental

Supported atomically dispersed Rh catalysts were prepared by a strong electrostatic adsorption method. Catalysts were characterized by a range of techniques, including UV-Vis and Raman spectroscopy, CO probe molecule infrared (IR), and transmission electron microscopy to understand the local structure and Rh charge state.

3. Results and Discussion

Figure 1 (a) and (b,c) show representative image of the Rh/ReO_x-Al_2O_3 and corresponding line scan intensity analysis of the two selected dimers, respectively. The difference in scattering intensity of Rh and Re species due to their different atomic mass (intensity α $Z^{1.5\text{-}2}$, where Z represents atomic number) evidences the formation of Rh-ReO_x atomically dispersed site pairs in Rh/ReO_x-Al_2O_3.

For ethylene hydroformylation, the propanal formation was greatly enhanced over Rh/ReO_x-Al_2O_3 and Rh/WO_x-Al_2O_3 relative to Rh/Al_2O_3, resulting in the higher selectivity toward propanal up to 63%. Interestingly, the selectivity toward propanal substantially changed depending on WO_x structure nearby dispersed Rh species. When Rh were localized with atomically dispersed WO_x (Rh/1WO_x-Al_2O_3), the selectivity toward propanal is the higher (63%) than Rh on bare Al_2O_3 (Rh/Al_2O_3, 22%), a polystungstate monolayer (Rh/2WO_x-Al_2O_3, 43%) and monoclinic WO_3 crystallites (Rh/8 and 25WO_x-Al_2O_3, 50%).

Kinetic experiments revealed that Rh/ReO_x-Al_2O_3 and Rh/WO_x-Al_2O_3 have higher CO reaction orders relative to Rh/Al_2O_3, indicating a decrease in the CO binding energy on Rh in Rh-ReO_x and Rh-WO_x co-localized structures, which was further evidence by CO temperature program desorption (TPD) characterization. This suggests that the promoted reactivity for Rh/ReO_x-Al_2O_3 and Rh/WO_x-Al_2O_3 was primarily due to an increase in the concentration of vacant sites under reaction conditions. As shown in Figure 2, the CO reaction orders increased and became positive over Rh/1 and 3WO_x-Al_2O_3, potentially suggesting that C_2H_4 adsorbed on atomically dispersed WO_x reacts with CO on nearby dispersed Rh. Two classes of active sites consisting of Rh and WO_x with an atomic intimacy allow a cooperative bifunctional mechanism when Rh is coordinated with atomically dispersed WO_x, consistent with previous report studies reporting atomically dispersed WO_x as active sites for olefin metathesis.

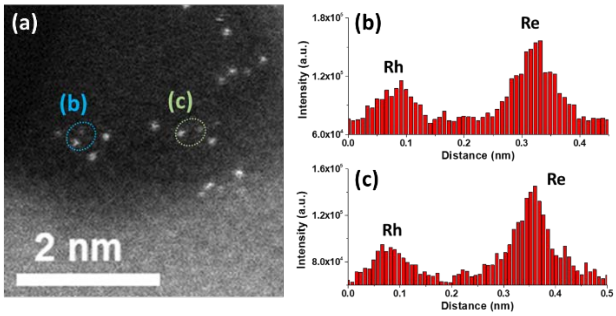

Figure 1. (a) HAADF STEM image of Rh/ReO_x-Al_2O_3. (b,c) Corresponding line scan intensity analysis of the two selected dimers shown in (a).

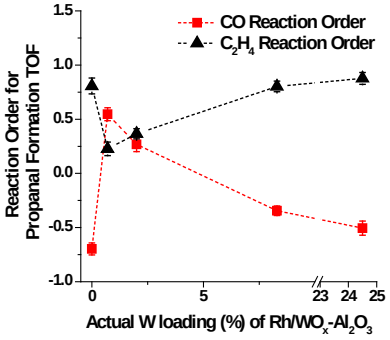

Figure 2. CO and C_2H_4 reaction orders for propanal formation TOF as a function of actual W loading of Rh/WO_x-Al_2O_3.

インターナショナル sess.

[1A11-13] インターナショナル sess.(2)

座長:比護 拓馬(早稲田大学)

2021年11月11日(木) 14:15 〜 15:00 A会場 (函館アリーナ 会議室A)

[1A11] ゼオライト内インジウムヒドリド種の局所構造とエタン脱水素化能

○安村 駿作[1]、鳥屋尾 隆[1,2]、前野 禅[1]、清水 研一[1,2] （1. 北海道大学触媒科学研究所、2. 京都大学触媒電池）

14:15 〜 14:30

[1A12] Au-Pt/ゼオライトを用いた0℃における高効率エチレン除去

○Lin Mingyue[1]、Wang Haifeng[1]、宍戸 哲也[1]、三浦 大樹[1]、春田 正毅[1]、村山 徹[1,2] （1. 東京都立大学、2. 煙台大学）

14:30 〜 14:45

[1A13] Catalytic reduction of NO to ammonia by CO-H_2O over metal oxide supported catalysts

○Chaudhari Chaudhari Chandan[1], Keisuke Kobayashi[1], Yuichi Manaka[1,2], Tetsuya Nanba[1] （1. Fukushima Renewable Energy Inst., AIST , 2. Tokyo Inst. Tech. ）

14:45 〜 15:00

Local structure of In-hydride species in zeolite and its reactivity for C_2H_6 dehydrogenation

(Institute for catalysis, Hokkaido University* · Elements Strategy Initiative for Catalysts & Batteries (ESICB), Kyoto University**)○Shunsaku Yasumura*, Takashi Toyao*,**, Zen Maeno*, Ken-ichi Shimizu*,**

1. Introduction

Hydrides in/on solid materials have attracted significant attention in many research fields, including energy engineering, electrochemistry, and catalysis. Research on the synthesis, characterization, and catalytic function of the isolated surface hydrides is an attractive but formidable task.[1] In this study, in-situ IR and DFT calculation were carried out to find the formation of isolated In-hydride species in indium-exchanged CHA zeolite (In-CHA).[2] The catalytic ability of In-CHA on C_2H_6 non-oxidative dehydrogenation was examined, resulting in superior selectively (96 %) and low coke formation during a long-term reaction (90h). By the combination of kinetic analysis and transition state (TS) calculation, it was elucidated that its catalytic performance was originated from the formation of not mono-hydride ($[InH]^{2+}$) but di-hydride species ($[InH_2]^{+}$) as active sites.

2. Experimental

In_2O_3 supported on the proton-type CHA (In_2O_3/CHA) was synthesized through impregnation of $In(NO_3)_3 \cdot nH_2O$ (Kanto Chemical Co., Inc.) in the NH_4^+-type CHA zeolite (Tosoh, SiO_2/Al_2O_3 = 22.3), followed by drying in an oven and calcination under air for 1 h at 773 K. Afterward, the reductive solid-state ion-exchange reaction of In_2O_3/CHA was conducted in the presence of H_2 at 773 K. For IR spectroscopic experiments, the In-CHA disk was prepared in-situ in a quartz reactor from a self-supported disk of In_2O_3/CHA. DFT calculations were performed using the Vienna ab initio simulation package (VASP) with a periodic boundary condition under the Kohn−Sham formulation.

3. Result and Discussion

The in-situ IR measurement of In-CHA treated with H_2 at 773 K (In-CHA(H_2)) was performed. The IR spectrum of In-CHA(H_2) exhibited a band with a maximum at 1720 cm^{-1} (Figure 1a) arising from In−H stretching vibrations (ν(In−H)). This band remained unchanged even at 473 K. After H−D exchange reaction with D_2 at 373 K, ν(In−H) decreased and disappeared at 473 K. ν(In−H) appeared again by the following exposure to H_2 at 473 K. The gas-phase products were also analyzed by mass spectrometry during the H−D exchange reaction with an increase in the temperature from 313 to 473 K. The reaction of In-CHA(H_2) with D_2 afforded a positive peak for m/z = 3 with a negative peak for m/z = 4 around 373−473 K (Figure 1b), while a peak for m/z = 2 was hardly observed. A control experiment using proton-type CHA (H-CHA) instead of In-CHA (H_2-treated H-CHA with D_2) was conducted where no peak was observed for all signals, supporting the occurrence of an H−D exchange reaction between In-hydrides and D_2.

In-CHA exhibited high selectivity (96 %) and durability for the nonoxidative ethane dehydrogenation without cofeeding of H_2. The activity and selectivity of In-CHA were maintained for at least 90 h, and the catalyst was reusable without loss of its efficiency. Based on the results of kinetic analysis and TS calculations, the formation of $[InH_2]^+$ as active sites is responsible for the durable reaction due to the less formation of Bronsted acid sites and carbenium cations. More detailed reaction mechanisms and the relationship with the local structure of In-hydride species will be discussed

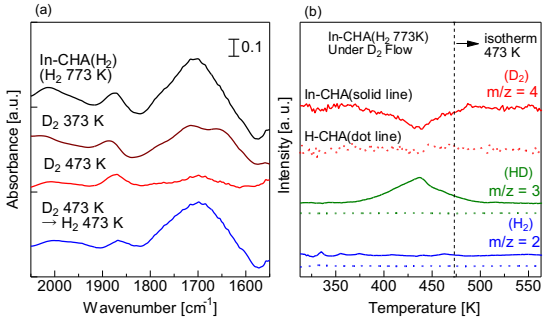

Figure 1 (a) FTIR spectra of In-CHA after H_2 treatment at 773 K (In-CHA(H_2)) and H−D exchange reactions. (b) Mass profiles for m/z = 2, 3, and 4 during H−D exchange reaction of In-CHA(H_2) (solid line) or H-CHA(H_2) (dot line) with D_2.

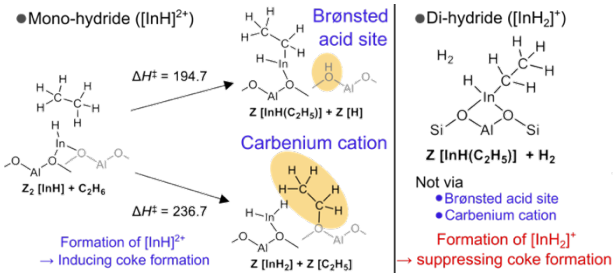

Figure 2 Reaction scheme of non-oxidative dehydrogenation of C_2H_6 on indium mono-hydride ($[InH]^{2+}$) and di-hydride ($[InH_2]^{+}$) species in zeolite.

References

1 C. Copéret, D. P. Estes, K. Larmier and K. Searles, *Chem. Rev.*, 2016, **116**, 8463.

2 Z. Maeno, S. Yasumura, X. Wu, M. Huang, C. Liu, T. Toyao and K. Shimizu, *J. Am. Chem. Soc.*, 2020, **142**, 4820.

Highly efficient removal of ethylene at 0 °C over Au-Pt/zeolite

([1]Tokyo Metropolitan University, [2]Yantai University)
○Mingyue Lin[*1], Haifeng Wang[*1], Tetsuya Shishido[*1], Hiroki Miura[*1], Masatake Haruta[*1], Toru Murayama[*1,2]

1. Introduction

Ethylene (C_2H_4) released from the plants could fasten the mature and deterioration of fresh fruits and vegetables even at low temperatures since it is a natural gaseous plant hormone. To prolong the storage time of the fresh plants during the transportation, removing trace amounts of C_2H_4 is important, and selective catalytic oxidation of C_2H_4 to CO_2 is an ideal method.[1] However, almost all of the reported catalysts would be deactivated due to the water adsorption, usually within 1 h. Therefore, it is necessary to develop a more effective material with a high C_2H_4 removal efficiency and long-term stability at low temperatures (0~5 °C).

Here, we report an Au-Pt/zeolite (ZHM20) with a highly active C_2H_4 removal efficiency (81%) and long-term stability (40 h) for C_2H_4 elimination at 0 °C.

2. Experimental

Mordenite 20 (ZHM20, SiO_2/Al_2O_3=18.3) provided by the Catalysis Society of Japan was used as the support. The loading amount of nanoparticles was prepared as 1wt%. Sol immobilization method[2] was applied to prepare ZHM20, Pt/ZHM20, Au/ZHM20, and Au_xPt_y/ZHM20 (x and y represent the molar ratio of Au and Pt, respectively) and they were calcined at 500 °C for 2 h before being used.

A fixed-bed flow reactor was used to conduct the C_2H_4 removal test. The sample (0.2 g) was firstly pretreated at 150 °C for 2 h under N_2 with a flow rate of 50 mL min^{-1} before being evaluated under the reactant gas that contained 50 ppm C_2H_4, 20% O_2, and N_2 balance with a total flow rate of 10 mL min^{-1}. The inlet and outlet concentrations of C_2H_4 and CO_2 were analyzed by an online 490 Micro GC system (Agilent) for calculating the removal efficiency of C_2H_4 and the yield of CO_2.

3. Results and Discussion

As shown in Figure 1, the initial C_2H_4 removal efficiency over ZHM20 was 100% at 0 °C and it reached the maximum adsorption capacity after flowing 11 h of 50 ppm C_2H_4. The removal efficiency curves of Pt/ZHM20 and Au/ZHM20 were U-shaped. Initially, the removal efficiency was 100% and it decreased to 19% and 15% after 10 h-on-stream over Pt/ZHM20 and Au/ZHM20, respectively, which was the same with that observed from ZHM20, suggesting that this step might be owing to the adsorption of C_2H_4 on ZHM20. Then, the C_2H_4 removal efficiency increased until reaching the steady-state of 56% on Pt/ZHM20 and 45% on Au/ZHM20. $Au_{54}Pt_{46}$/ZHM20 also showed a U-shape removal efficiency curve, but the turning point time of 3.5 h was much shorter than the other two. Moreover, the C_2H_4 removal efficiency of $Au_{54}Pt_{46}$/ZHM20 at the steady-state was 81% and it lasted for as long as 40 h. According to the electronic state analysis, $Au_{54}Pt_{46}$/ZHM20 possessed electron-deficient Pt species and electron-rich Au species, which might be helpful for the faster adsorption and transformation of C_2H_4 on $Au_{54}Pt_{46}$ NPs than that on Au NPs and Pt NPs.

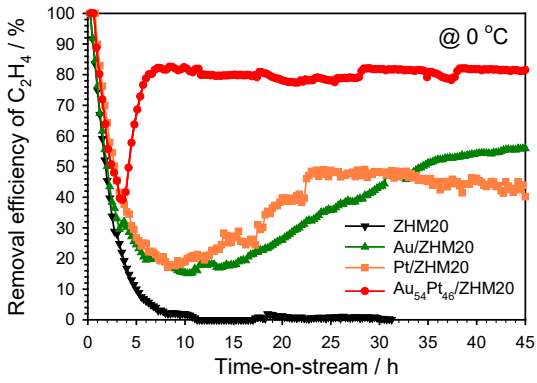

Figure 1. The removal efficiency of C_2H_4 with time-on-stream over ZHM20, Au/ZHM20, Pt/ZHM20, and $Au_{54}Pt_{46}$/ZHM20 at 0 °C.

1) C. Jiang, K. Hara, A. Fukuoka, Angew. Chem. Int. Ed., 52(24), 6265 (2013)
2) H. Miura, Y. Tanaka, K. Nakahara, Y. Hachiya, K. Endo, T. Shishido, *Angew. Chem. Int. Ed.*, 130(21), 6244 (2018)

Catalytic reduction of NO to ammonia by H_2 or CO-H_2O over metal oxide supported catalyst.

(FREA[1], TIT$_2$) ○C. Chaudhari,[1] K. Kobayashi,[1] Y. Manaka[1,2*] T. Nanba[1]

1.Introduction

Ammonia is an important *N*-containing chemical which is used as fertilizer, starting material for heterocycles sthe synthesis and carbon-free fuel. Ammonia is synthesized industrially by Haber-Bosch method with high energy consumption. Ammonia synthesis from air pollutant NO is an attractive alternative to reduce the concentration of NO. Several reductants such as hydrocarbon, H_2 or CO-H_2O have reported for the transformation of NO to NH_3. Recently, our group developed Pt/TiO_2 catalyst for ammonia synthesis on NO-CO-H_2O reaction.[1] However, the activity of Pt/TiO_2 was not studied for NO-H_2 reaction. In this study, we investigated and optimized the catalytic activity of Pt/TiO_2 for NH_3 synthesis. Furthermore, the activity of Cu/CeO_2 catalyst at lower temperature (>200 °C) investigated for NO-CO-H_2O reaction.

2. Experimental

Supported metal catalysts were prepared by an incipient wetness method with different Pt or Cu precursors. TiO_2 or CeO_2 support was prepared by sol-gel method using different conditions. All catalysts were characterized by BET and CO adsorption. The catalytic activity was measured by a fixed-bed flow reactor. For NO-H_2 reaction, the feed gas was composed of 0.1 % NO, 0.3% H_2 ppm with dilution by Ar. For NO-CO-H_2O reaction, the feed gas was composed of 0.1 % NO, 0.3% CO and 1% H_2O ppm with dilution by Ar. The total flow was set to 250 mL/min. The product gases were analyzed online Fourier transform infrared spectroscopy and gas chromatography.

3. Results and Discusion

Initially, we synthesized Pt/TiO_2 catalyst using different precursor such as $(NH_3)_4Pt(NO_3)_2$, $(NH_3)_4Pt(Cl)_2$, $(NH_3)_4Pt(OH)_2$ and H_2PtCl_6 and tested for NO-H_2 reaction. All precursors showed full conversion (100 %) of NO. The catalytic activity of all four precursors for ammonia selectivity was almost similar at lower temperature (100 °C-150 °C). When the temperature increased to 230 °C, H_2PtCl_4 showed superiority (99 %) for the synthesis of ammonia (Fig.1). Later, we investigated the effect of reduction temperature using different temperatures (400 °C, 500 °C and 600 °C). When Pt/TiO_2 catalyst prepared from H_2PtCl_4 precursor reduced at 400 °C, high yield of ammonia (98.9%) was obtained at 230 °C.

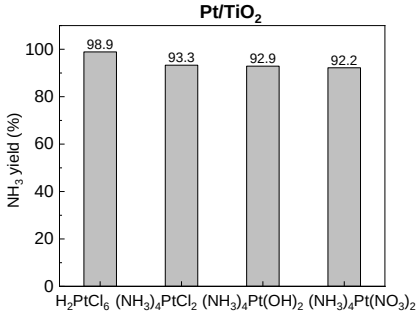

Fig. 1. The activity of Different Pt catalysts at 230 °C

For NO-CO-H_2O reaction, we examined Cu/CeO_2 catalysts prepared from different precursors at 150 °C. The catalyst prepared from $Cu(NO_3)_2$ precursor showed higher yield (72%) than other precursors.

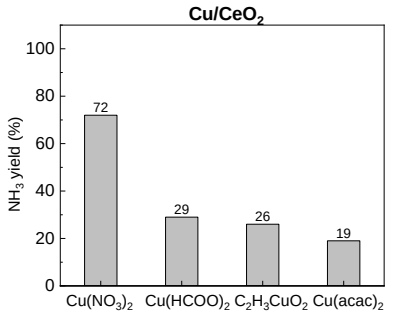

Fig. 2. The activity of Different Pt catalysts at 150 °C

In summary, Pt/TiO_2 prepared from H_2PtCl_6 found to be an active catalyst for ammonia synthesis over NO-H_2 reaction. In NO-CO-H_2O reaction, Cu/CeO_2 catalyst showed high activity for ammonia synthesis.

[1]K. Kobayashi, R. Atsumi, Y. Manaka, H. Matsumoto, T. Nanba, *Catal. Sci. Technol.,* **9**, 289 (2019).

インターナショナル sess.

[1A14-16] インターナショナル sess.(3)

座長:桑原 泰隆(大阪大学)

2021年11月11日(木) 15:15 〜 16:00 A会場 (函館アリーナ 会議室A)

[1A14] Low-temperature conversion of methane to methanol using carbon nanotubes supported catalyst

○Yingluo He[1], Guohui Yang[1], Noritatsu Tsubaki[1] （1. University of Toyama）

15:15 〜 15:30

[1A15] CO_2吸着用 HKUST-1モノリスのワンポット合成

○酒井 求[1]、堀 隼太[2]、伊藤 綾香[3]、松本 隆也[4]、朝野 剛[4]、松方 正彦[1,2,3,5] （1. 早稲田大学ナノ・ライフ創新研究機構、2. 早稲田大学大学院先進理工学研究科応用化学専攻、3. 早稲田大学先進理工学部応用化学科、4. ENEOS株式会社、5. 早稲田大学理工学術院総合研究所）

15:30 〜 15:45

[1A16] 火炎噴霧熱分解法により調製した Zr添加 Ni/CeO_2の CO_2メタン化反応活性

○藤原 翔[1]、樫野 宗悟[1]、吉岡 大[2] （1. 山形大学大学院　理工学研究科、2. 山形大学　工学部）

15:45 〜 16:00

Low-temperature conversion of methane to methanol using carbon nanotubes supported catalyst

(University of Toyama) ○Yingluo He, Guohui Yang, Noritatsu Tsubaki

1. Introduction

Conversion of methane to methanol is performed by a two-step process under harsh reaction conditions in industry. The direct synthesis process of methanol from partial oxidation of methane has been studied for a few decades. However, it remains one of the considerable challenges in the sector of methane utilization. [1] Herein, we report carbon nanotubes (CNTs) supported palladium-gold (Pd-Au) nanoparticles catalyst for this direct synthesis, which shows outstanding methanol selectivity and productivity at low temperature. [2), 3)]

2. Experimental

2.1 Catalyst preparation

Commercial CNTs were pretreated by various acids to modify its surface properties. The supported Pd-Au catalysts were prepared by an incipient wetness impregnation method. The Pd and Au amount were 2.5 % wt respectively without explain.

2.2 Catalyst characterization

XRD, XPS, H_2-TPR, CO-PULSE, FE-SEM, HR-TEM measurements were performed to analyze the physical and chemical properties of our catalysts.

2.3 Catalytic tests

Catalyst tests for direct synthesis of methanol from methane were accomplished in a stainless-steel autoclave. The motor was vigorously stirred at 1200 rpm, the temperature was raised to 50 °C to start the reaction at the same time. After the 30 min reaction, the vessel was cooled by ice (< 10 °C), to avoid volatilization of the products.

3. Results and Discussion

The carbon materials such as carbon nanotubes (CNTs), activated carbon (AC), and reduced graphene oxide (rGO) are employed as the catalyst support, and the palladium-gold (Pd-Au) nanoparticles are used as active center. By using oxygen/hydrogen mixture as oxidant in the direct synthesis, it is found that Pd-Au/CNTs catalyst shows outstanding methanol selectivity and productivity.

Table 1 Catalytic performance with different carbon supported Pd-Au nanoparticles catalyst

Catalyst	Total product ($mmol/kg_{cat.}$)	MeOH Selectivity (%)	TON of MeOH [b]
Pd-Au/rGO	33.2	54.2	76.5
Pd-Au/AC	156.0	65.6	435.1
Pd-Au/CNTs	190.1	73.2	591.7
Pd-Au/CNTs-a	149.5	71.2	452.6
Pd-Au/CNTs-n	98.0	90.0	375.0

a: Reaction conditions: Time 30 min; Temp. 50 °C; Solvent H_2O 10 mL; Catalyst weight 30 mg; Feed gas $CH_4/O_2/H_2/Ar$; Total pressure 3.3 MPa.
b: mmoles of MeOH formed by per mole Pd metal.

Compared with the Pd-Au/CNTs, the Pd-Au/CNTs-n catalyst with a treatment of nitric acid on the CNTs support enhances the methanol selectivity obviously (Table 1), due to the changed surface oxygen species on the supports. In addition, our characterization results reveal that a weak interaction between Pd-Au nanoparticles and CNTs support is in favor of methanol productivity and selectivity.

This work offers a simple and effective strategy to directly synthesize methanol from methane partial oxidation under the mild conditions.

1) Hammond C, Forde M. M, Ab Rahim M. H, et al.; *Angew. Chemie - Int. Ed.*, **51**, 5129 (2012).
2) He Y, Luan C, et al.; *Catalysis Today*, **339**, 48 (2020).
3) He Y, Liang J, et al.; *Catalysis Today*, **352**, 104 (2020).

One-pot synthesis of HKUST-1 monolith for CO_2 adsorption

CO_2吸着用 HKUST-1 モノリスのワンポット合成

(早大ナノ・ライフ*・早大先進理工**・ENEOS 株式会社***・早大理工総研****)
○酒井 求(さかいもとむ)*・堀隼太(ほりはやた)**・伊藤綾香(いとうあやか)**・松本隆也(まつもとたかや)***・朝野 剛(あさのつよし)***・松方正彦(まつかたまさひこ)*, **, ****

1. Introduction

Metal-organic-framework (MOF) is drawn attention as CO_2 adsorbent. Shape forming technology for powdery MOF is required in order to generate objects of millimetric dimensions with enough mechanical resistance for application in industry[1]. In this study, alumina tube and Cu cube were used as the metal source for MOF preparation and a part of them was directly converted into MOF monoliths. The preparation method of MOF monolith and its adsorption property were investigated.

2. Experimental

Two types of monoliths containing MOFs, HKUST-1 and MIL-96, were prepared. HNO_3, trimesic acid (TMA), and porous α-alumina tube were used as raw materials for MIL-96 preparation. Porous Cu cube was used for HKUST-1 preparation instead of α-alumina tube. Either alumina tube or Cu cube was placed into the aqueous solution of HNO_3 and TMA, and then hydrothermally treated by using glass-lined autoclave. The effect of these preparation conditions on the preparation of MOF monolith was studied.

MIL-96 powder was synthesized according to the literature[2] as reference material. HKUST-1 powder (Basolite C-300) was purchased from Sigma-aldrich.

CO_2 adsorption properties of prepared MOF powder and monoliths were measured by volumetric adsorption method (Belsorp-MAX, microtracBEL).

3. Results and discussion

The concentrations of HNO_3 and TMA and the conditions of hydrothermal treatment were widely changed. By the optimization of synthesis conditions, the contents of MIL-96 and HKUST-1 in monoliths increased up to 6.0 and 32 wt%, respectively.

Fig. 1 shows the morphological features of raw materials of metal sources and monoliths synthesized. The surface of alumina tube was fully covered with MIL-96 crystals and the color of alumina tube changed to yellow. The surface of Cu cube was converted to HKUST-1 as well.

Fig. 2 shows the isotherms of CO_2 on MIL-96 and HKUST-1 monoliths and powders at 298 K. The adsorbed amount of CO_2 at 100 kPa on MIL-96 monoliths and powder were 140 and 95 cm^3(STP) g^{-1}, respectively. HKUST-1 powder and monolith showed almost the same values of the CO_2 adsorbed amount, 99 cm^3(STP) g^{-1}.

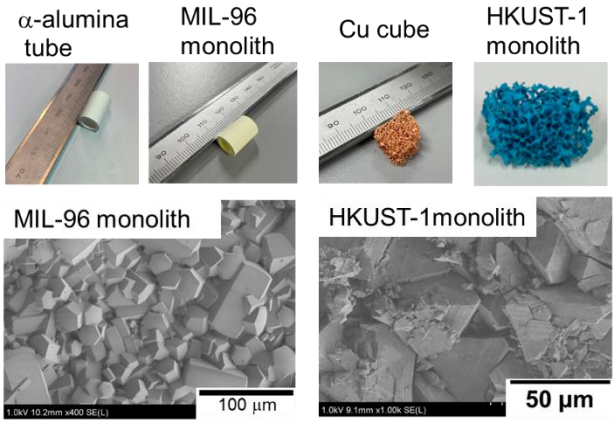

Fig. 1 Typical photo and FE-SEM images of α-alumina, MIL-96 monolith, Cu cube and HKUST-1 monolith.

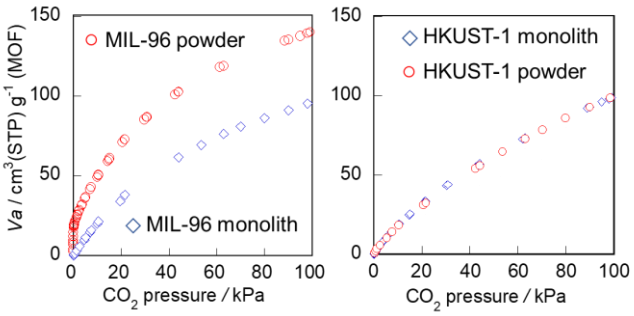

Fig. 2 CO_2 isotherms on MIL-96 and HKUST-1 at 298 K.

References

1) Bazer-Bachi, D., *et al., Powder Technol.*, **255** (2014) 52-29.
2) Benoit, V. *et al., J. Mater. Chem. A*, **6** (2018) 2081-2090.

Zr doped Ni/CeO_2 prepared by Flame spray pyrolysis for CO_2 methanation

(Yamagata University) Kakeru Fujiwara*, Syugo Kayano and Dai Yoshioka

1. Introduction

Utilization of CO_2 by converting it into CH_4 is sought because it reduces CO_2 emission to the environment and stores H_2 produced by renewable energies. So far, for this reaction, Ru supported on CeO_2 is one of the most active catalyst but its utilization is limited due to the cost of Ru. Alternatively, Ni has attracted the interest but it suffers from the low activity at low temperature (< 250 ºC) compared to Ru catalysts. To address the issue, high Ni loading with keeping the size small is promising approach for maximizing the Ni surface area. Here, we successfully prepared highly-loaded NiO (60 wt% as Ni) on CeO_2 nanoparticles by flame spray pyrolysis (FSP). Furthermore, the effect of Zr doping to the Ni/CeO_2 catalyst for CO_2 methanation was investigated.

2. Experimental

Ni (60wt%) supported on $Ce_{1-x}Zr_xO_2$ (x = 0 and 0.1) was prepared by an FSP reactor [1]. Appropriate amount of Ni (II) acetate tetrahydrate (Wako, purity > 98.0%), Zr 2-ethylhexanoate in mineral spirits (Wako, 11.7-12.3% as Zr) and Ce (III) 2-ethylhexanoate, 49% in 2-ethylhexanoic acid (Alfa Aesar, Ce: 12%) were mixed with a mixture (1: 1) of 2-ethylhexanoic acid (Sigma-Aldrich, purity > 99%): methanol (Wako, Reagent Grade) to be the total metal concentration (Ni + Zr + Ce) of 0.2 M. The precursor solution was fed to the two-fluid spray nozzle at 3 mL min^{-1}, dispersed to a fine spray by 5 L_{STP} min^{-1} of O_2 dispersant (technical grade). The spray was evaporated and combusted by a premixed CH_4/O_2 plot flame (1.5 L_{STP} min^{-1}/3.2 L_{STP} min^{-1}) to form particles. The particles were collected on a glass-fiber filter by a vacuum pump (Busch SV1040C). Also, 20 and 60 wt% of Ni was deposited on FSP-made pure CeO_2 by an impregnation method. Before the characterization and activity tests, all the catalysts were reduced in 5%H_2-Ar at 500°C for 1 h.

Catalytic activity was evaluated using a fixed bed reactor. The catalyst (100 mg) and SiC powder (400 mg) were filled into a quartz tube (inner/outer diameters of 6/8 mm). The catalyst was reduced at 500 °C for 1 h in 5% H_2–Ar (100 mL_{STP} min^{-1}), and subsequently, a reactant gas ($CO_2/H_2/N_2$ = 1/4/1) was fed to the catalyst at 60 mL_{STP} min^{-1}. The composition of the product was measured by a gas chromatograph equipped with a thermal conductivity detector.

3. Results and discussion

PXRD pattern of all the catalysts shows the peaks of fluorite CeO_2 at 28° and 33°. In the absence of Zr, the peak potions were identical while the Zr doping shifts the peaks to the higher diffraction angle. Additionally, the peaks of monoclinic and tetragonal ZrO_2 were not detected. These facts indicate the preferable Zr doping to the CeO_2 lattice. EDX mapping (not shown) exhibited the size of Ni in FSP-made 60Ni/CeO_2 and 60Ni/$Ce_{0.9}Zr_{0.1}O_2$ was small (10-20 nm), despite the high Ni content (60 wt%).

Figure 2 shows the activity of FSP-made and wet-made catalysts for CO_2 methanation. The conversion of FSP-made 60Ni/CeO_2 was higher than that of wet-made ones. Notably, the Zr doing by FSP significantly enhanced the catalytic activity. In addition, by-product (CO) was not detected for all the tests. In conclusion, highly active and selective catalyst was developed by simultaneously achieving high Ni content (60wt%), small Ni size (10-20 nm) and Zr doping to CeO_2 by FSP.

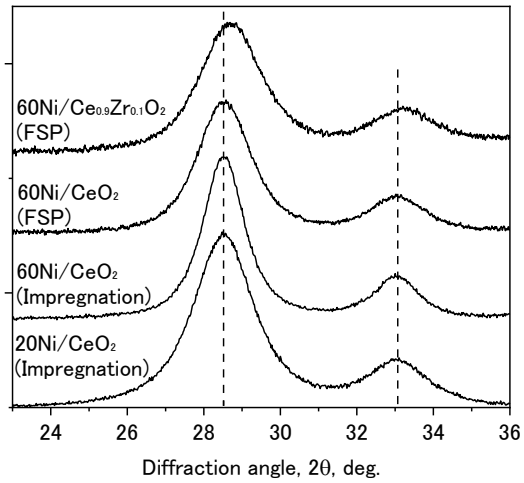

Fig. 1 PXRD patterns of FSP-made Ni/$Ce_{1-x}Zr_xO_2$ and wet-made Ni/CeO_2 particles

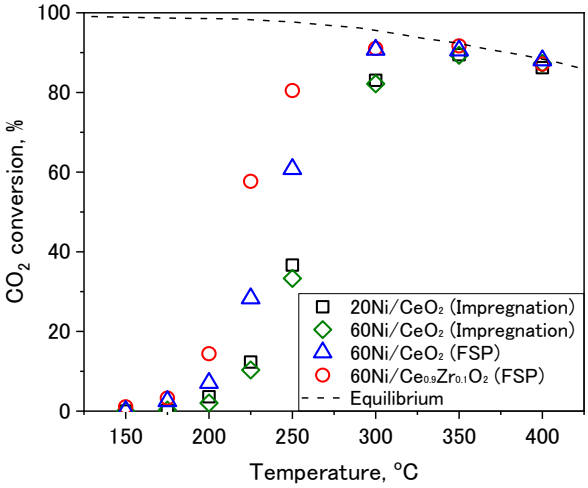

Fig. 2 Catalytic activity of FSP-made and wet-made catalysts for CO_2 methanation.

References

1. Fujiwara, K.; Tada, S.; Homma, T.; Sasaki, H.; Nishijima, M.; Kikuchi, R., AlChE *J.* **2019**, 65, e16717.

